# Definition and validation of a patient-individualized physiologically-based pharmacokinetic model

Roberto Andrea Abbiati[a], Gaetano Lamberti[b], Mario Grassi[c], Francesco Trotta[d], Davide Manca[a*]

[a]*PSE-Lab*, Process Systems Engineering Laboratory, Dipartimento di Chimica, Materiali e Ingegneria Chimica "Giulio Natta", Politecnico di Milano, Piazza Leonardo da Vinci 32, 20133 Milano, ITALY
[b]Dipartimento di Ingegneria Industriale, Università degli studi di Salerno, Via Giovanni Paolo II 132, 84084 Fisciano Salerno, ITALY
[c]Dipartimento di Ingegneria ed Architettura, Università di Trieste, Via Alfonso Valerio 6/A, 34127 Trieste, ITALY
[d] UO Chirurgia Generale e Toracica, Ospedale Maggiore di Lodi, Via Fissiraga 15, 26900 Lodi, ITALY

**ABSTRACT**: Pharmacokinetic modeling based on a mechanistic approach is a promising tool for drug concentration prediction in living beings. The development of a reduced physiologically-based pharmacokinetic model (PBPK model), is performed by lumping organs and tissues with comparable characteristics respect to drug distribution phenomena. The proposed reduced model comprises eight differential equations and 18 adaptive parameters. To improve the quality of the PBPK model these adaptive parameters are alternatively: (i) individualized according to literature correlations on the physiological features of each patient; (ii) assigned as constants based on the features of either human body or drug properties; (iii) regressed respect to experimental data.

The model predictive capability is validated with experimental blood concentrations of remifentanil, an analgesic drug, administered via bolus injection with four doses (2, 5, 15, 30 μg/kg) to mixed groups of patients. Concentration profiles for the four simulated doses reveal a rather good consistency with experimental data.

*Corresponding author, phone +39 02 23993271, e-mail: davide.manca@polimi.it

# 1    Introduction

The administration of drugs to patients is one of the main activities involving physicians and this practice is matter of great attention. The discrimination among similar drugs to determine the most suitable one for a specific treatment and a given patient is rather challenging. Furthermore, the dose selection to achieve a desired effect is critical as an excessive quantity may cause toxic effects in patients whilst a moderate dose does not produce any benefits.

Dose appraisal related to the administration of anesthetics and analgesics during surgeries results particularly difficult. The anesthetist has to maintain the drug concentration in the blood amidst a well-defined range, called therapeutic window, to keep the patient sedated.

An important support to pharmaceutical companies during new-drug-development phases and to physicians in their daily activities can be provided by the application of mathematical models capable of describing the drug administration and biodistribution in the organism.

Pharmacokinetic (PK) modeling has been already applied to the pharmaceutical field and it allows scientists to determine the dynamics of blood drug concentration. Compartmental pharmacokinetic modeling can also be used to determine the drug PK parameters, such as the area under the curve ($AUC$), the terminal half-life time ($t_{1/2}$), and the clearance ($CL$) which support the physicians in administering the drug to patients properly.

In their native conception, classical compartmental pharmacokinetic (CCPK) models assumed that the human body could be depicted as a single volume, or compartment, to which the drug is administered and from which is eliminated. Those models were obtained by fitting exponential functions that depended on some parameters that did not have any physiological affinity to the human body and were only meant to minimize the error respect to experimental data (see Wagner (1981) for a review on the history of early PK modeling).

More recently, CCPK models were characterized by preserving a rather simplified approach, although the number of compartments increased (generally to two or three), and took into account, at different levels of detail, the connections among compartments (Wagner, 1993). These CCPK models carried along a series of drawbacks, the most important being the extreme simplicity of the model structure that hindered any direct correlation to real living systems. Therefore, every CCPK parameter had to be determined mathematically for every specific drug by a fitting procedure (*i.e.* (non)linear regression) respect to experimental data. As a consequence, CCPK models require conducting extended and differentiated studies on either humans or animals. These tests are expensive and ethical issues are always a matter of great concern. In addition, it is often challenging to scale up to humans the experimental activity conducted on animals (Mordenti, 1986; Jones and Rowland, 2013).

Recently, a contribution to the use of CCPK models was provided by Laínez-Aguirre *et al.* (2014), who proposed a model having a flexible structure. Based on an experimental data set, the model can reshape itself mathematically to produce a more suitable structure for the description of the specific pharmacokinetics under study.

A modern and alternative approach to pharmacokinetic modeling is based on the attempt to increase the mechanistic foundations by referring to and reproducing the real anatomy and physiology of mammalian systems. This is achieved by implementing an extended system of interconnected compartments. Here a compartment is an element that stands for either an organ or a tissue of the human/mammalian body, and which is mathematically described by a dynamic mass balance. By doing so, it is possible to quantify the concentration of the drug in blood, and in different organs and tissues. These mathematical *mockups* of mammalian body are named Physiologically Based Pharmacokinetic (PBPK) models.

A PSE-Lab publication

The transition from CCPK to PBPK models is justified by a number of advantages. In fact, the possibility to have a complete and detailed model of the human body to run *in silico* simulations of drug's ADME processes (*i.e.* absorption, distribution, metabolism, excretion) allows speeding up the development of new drugs by saving large amounts of money, shortening pre-clinical and clinical tests, and reducing the number of experiments on both animals and humans. The implementation of these models is not only important for pharmaceutical companies but also for physicians in several therapies and for patients' treatment (Egan, 2003).

This approach is favorably seen and progressively encouraged by pharmaceutical companies that start considering and referring to PBPK models in dossiers submitted to the regulatory agencies (Zhao *et al.*, 2012; Huang *et al.*, 2013).

## 1.1   ADME phenomena

The theoretical bases of physiological approach to PK modeling point to the mathematical reproduction of ADME processes. Drugs are administered to the organism via several routes (*e.g.*, enteral, parenteral, inhalation, topical). Each of these paths carries along a series of advantages and drawbacks. For instance, amongst the parenteral routes, the endovenous infusion is of common use. It guaranties an immediate introduction of the drug into the systemic circulation and the entire dose administered is available to produce the pharmacological effect. Despite these advantages, injections are often rejected by patients and are hardly applicable in case of self-administration. Either the oral (enteral route) or the transdermal (topical route) administrations are generally preferred, although they exhibit some disadvantages. In general, an orally-administered drug needs a delivery system capable of preserving the active principle when it crosses the gastric lumen and is eventually released in the intestine. In addition, the absorption is never complete and a fraction of the dose is expelled directly as unabsorbed. Several factors influence the intestinal absorption. They include gastric and intestinal pH, drug formulation, solubility, residence times in the lumina, simultaneous presence of food, and health condition.

Once the drug reaches the blood, it is conveyed in nearly every site of the organism by the circulatory system. The heart promotes the blood circulation along the arteries to the capillaries network and then back via the veins. When the drug reaches the capillaries, it can diffuse across blood channel walls into the interstitial liquid of tissues and subsequently to specific cells. This diffusive process may be either spontaneous (*i.e.* simply governed by concentration gradients) or promoted by specific transport mechanisms at the cell membrane surface.

Another important aspect, which limits the drug distribution process, is that drugs may bind to plasma proteins, typically human serum albumin, lipoproteins, and globulins. When the drug gets bound, it cannot leave the blood system and simply diffuse to organs, since the mass transfer phenomena are prevented for the protein-drug ensemble. This is a distinctive issue that has to be carefully considered when selecting the dose to be administered.

Being molecules, the active principles may undergo reactions occurring at different locations of the organism, to give metabolites. Metabolism plays an important role in drug elimination with reacted drugs having often low, if not negligible, pharmacological effects. The liver is the main site for metabolic reactions in the organism, but further reactions may occur also in the intestine, plasma, and tissue cells. Eventually, the drug is excreted from the organism. This occurs mainly via glomerular filtration of plasma in the kidneys with production of urine or via hepatic secretion into the bile. These mechanisms depend mainly on the molecular weight, the hydrophilicity value, and the ionization rate of drugs.

## 1.2   State of the art of PBPK modeling

Teorell's work (1937) was the progenitor of the PBPK approach to modeling. Despite that early production, the mechanistic approach took time to be accepted by the scientific community and some works were published only in the seventies of last century (Himmelstein and Lutz, 1979). The eighties saw a fast growth in the number of publications on the PBPK theme. In particular, Jain *et al.* (1981) proposed a complete whole-body PBPK model for the rat comprising 21 compartments and a system of 38 ordinary differential equations (ODEs) with 98 parameters, 37 of which had to be fitted by a regression procedure. Clearly, the application of that complicated and specialized system on one hand described in detail the rat's body but on the other hand was mathematically too heavy, with the burden of parameters evaluation hardly acceptable. As a matter of facts, a model overparameterization introduces the risk of perfectly identifying the experimental data used to determine the unknown parameters by a regression technique. This apparently perfect system identification would avoid spotting out possible experimental outliers (*aka* gross errors) and would specialize on the individual(s) used in the experimental campaign. The so high number of body variables described by Jain's model does not find an effective application even in case of experiments on animals. In fact, it is almost impossible to measure experimentally and dynamically the 38 body variables (for a consistent and exhaustive validation of that model) even working on rats that can be sacrificed and *measured* invasively. In addition, since a numerical or physiologically based scale-up procedure is not available to translate and port the model from rats to human beings (even in case of optimistic assignment and identification of all the 98 parameters) that model would remain tailored to the specific rats involved in the experimentation.

As a consequence, starting from the work of Jain *et al.* (1981), other PBPK models were proposed in the following years with the main goal of reducing the complexity while preserving as far as possible the physiological consistency. Some of these models still stand out today because they introduced new ideas and concepts. Yu *et al.*, (1996a,b) focused on the oral delivery and published a detailed model of the gastrointestinal tract, aimed at providing a mechanistic description of the absorption process. Based on ten compartments, the schematization of Yu and coworkers resulted highly detailed with an equivalent number of ODEs (*i.e.* 10) and 18 adaptive parameters. That model, named CAT (from Compartmental Absorption and Transit), showed an interesting agreement in humans with respect to experimental data for a series of active principles such as bretylium (Yu *et al.*, 1996a), sotalol (Yu *et al.,* 1996a), cefatrizine (Yu and Amidon, 1998), and atenolol (Yu and Amidon, 1999). Inspired by the CAT model, *Simulations Plus* (www.simulations-plus.com) introduced an improved version christened the ACAT (Advanced Compartmental Absorption and Transit) model. Such a model featured a detailed compartmental description of the gastrointestinal tracts (Agoram *et al.*, 2001), whose constituting equations are not available to the public as they are protected by copyright and commercialized as a standalone software (GastroPlus™).

More recently Pavurala and Achenie (2013) described a mechanistic approach specifically devoted to orally delivered drugs. In their work the CAT model is coupled to a drug dissolution one to describe in detail the drug release, absorption, and transit phases. Similarly, Grassi *et al*. (2010) and Del Cont *et al.* (2014) proposed a detailed model involving the physical processes that determine the release of drugs (in crystalline, nano-crystalline, and amorphous forms) from an ensemble of poly-dispersed, swelling, and not eroding polymeric particles.

Mošat' *et al.* (2013), proposed a whole-body PBPK model for the rat. Their software can automatically generate an ODE system, featuring a vascular network structure, and determine the best set of parameters that describe the cyclosporin pharmacokinetics via a least square minimization between the experimental and predicted drug concentration profiles (see also Heitzig *et al.*, 2014).

To reduce the structural and numerical complexity of the modeled system, a typical technique consists in lumping groups of compartments into a single one. By doing so, both organs and tissues, which behave similarly respect to drug distribution and are not required to be considered individually, can be merged into a lumped compartment. Complete and mathematically detailed descriptions of this modeling approach are available in Nestorov *et al*. (1998); Gueorguieva *et al.,* (2006); Pilari and Huisinga (2010).

The idea of clustering whole-body PBPK models into more simplified, although equally detailed models, gave rise to the term *minimal-PBPK* (Cao and Jusko, 2012). An interesting example of these PBPK models, characterized by a reduced complexity, is available in Di Muria *et al.* (2010) where a rather simplified, though complete mammalian structure, is obtained by modeling two lumped compartments, namely the plasma and the organs/tissues. The organs/tissues that are highly perfused by blood are lumped together with plasma in a larger compartment called Plasma. Likewise, the tissues that are less perfused by blood compose the so-called Tissues compartment. The PBPK model of Di Muria *et al.* (2010) counts seven compartments (*i.e.* gastric lumen, small intestine, large intestine, gastro intestinal circulatory system, liver, plasma, and tissues). The corresponding numerical formulation comprises 7 ODEs that represent the dynamic mass balances of lumped compartments, which exchange material flows according to the anatomy and physiology of human body.

Opting for a reduced model is favorable for a number of reasons. Firstly, there is a mathematical motivation related to the reduction in the number of uncertain parameters, which ought to be always kept low, and a limited computation time. This aspect might appear of secondary importance, but it plays a significant role in case of application to pharmacodynamic monitoring, specifically when applied online during patient therapy. Secondly, a more granular model should be justified by the availability of large sets of experimental data which unfortunately in most cases are not available, specifically in case of human studies. Thirdly, as one of the main reasons for PBPK modeling is animal to human translation, an extended and over parametrized model would hamper this extrapolation activity because of the differences in biological properties between species.

# 2 Methods

Laying the foundations on the work of Di Muria *et al.* (2010), this article proposes a new formulation of the PBPK model based on the *minimal*-approach theory of Cao and Jusko (2012) to describe the pharmacokinetics of active principles in the human body. For the sake of simplicity, this new model is identified by the mPBPK abbreviation which stands for minimal-PBPK.

Specifically, the paper deals with a case study based on the pharmacokinetics of remifentanil (an analgesic drug) to assess the predictive capability of the model. The experimental data used in the case study are reported in the papers of Egan *et al.* (1993) and Westmoreland *et al.* (1993) that show the dynamic trends of remifentanil concentration in the patients' blood at different administration doses. The proposed mPBPK formulation attempts to enhance the physiological fidelity of available PBPK models and suggests some expedients to increase the robustness of the numerical framework (see also Abbiati *et al.* (2015a,b) for further details about modeling the oral administration of drugs to mammals).

## 2.1 Model structure

Figure 1 shows the model structure that suggests a compromise between lumped compartments and single organs for the description of the pharmacokinetics of active principles. The mPBPK modeling philosophy exploits as far as possible the physiological consistency with the mammalian body and specifically with the

human one. This consistency, whenever possible, is pushed a step forward by evaluating some adaptive parameters of the model such as the physiological constants, which are personalized (*i.e.* individualized) according to the specific features of the patient's body. This Section discusses in detail the mPBPK model.
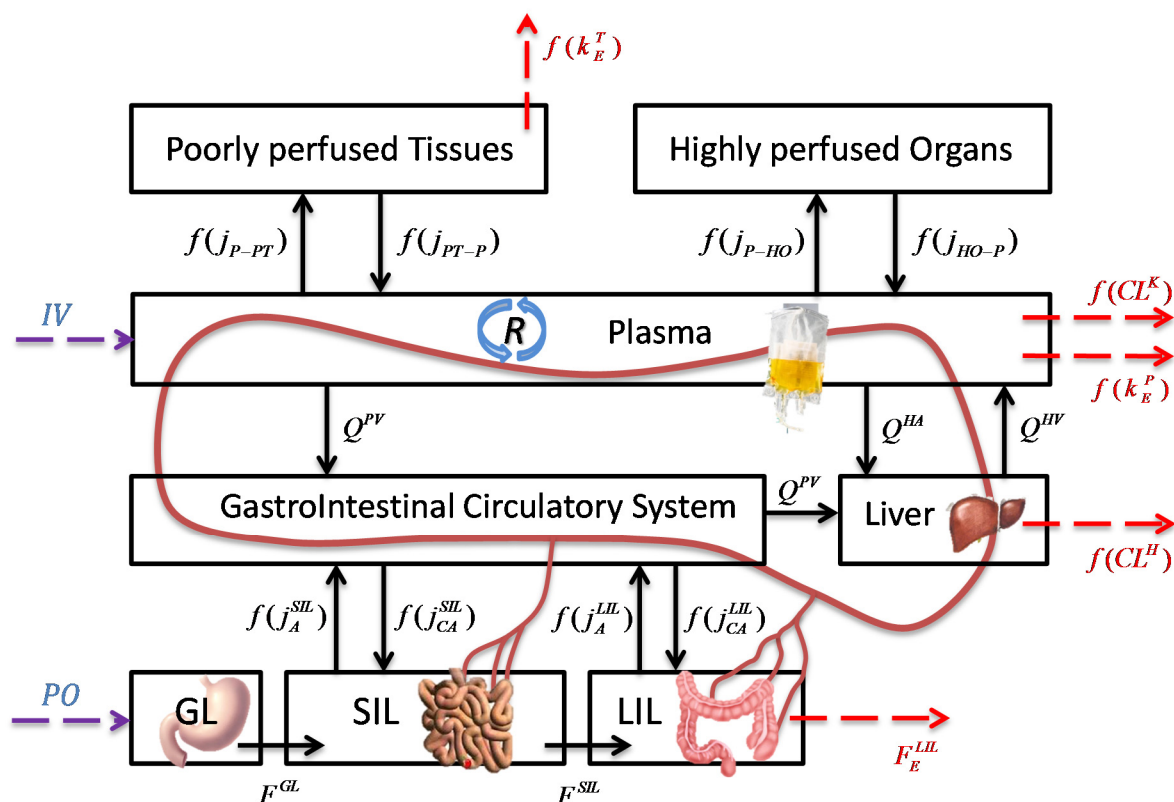


Figure 1: Structural definition of the proposed mPBPK model. Rectangular boxes represent either single or lumped organs/tissues. The dark red Bezier curves symbolize the blood circulation system, which reaches the gastro-intestinal region through the gastro-intestinal circulatory system. $IV$ (intravenous) and $PO$ (oral) are two possible administration routes, while the red arrows are the excretion routes, which are functions, $f$, of the specific elimination paths. $R$ accounts for the process of drug binding to proteins in plasma, which affects severely the distribution process. The mathematical setup is described by equations (1-8). See both Table 1 and Notation for a more accurate description of symbols, parameters, and units of measure.

To provide a physiological description of the mPBPK model, we follow the path of the drug when it is assumed orally, as this is the path that involves more organs before entering the plasma. We will first focus on the gastrointestinal region, where the drug dissolves in the stomach and is absorbed through the intestinal wall into the gastrointestinal circulatory system. This system delivers the drug to the liver and later to the central circulatory system, as Plasma compartment takes the drug to all the other organs and tissues. The drug is eventually eliminated through different routes, which are metabolism (*i.e.* chemical reaction) and excretion of the original molecule (*i.e.* via urine, bile, or faeces). With reference to these basic steps, we provide an accurate description of both physiological and biological aspects of interest, together with the mathematical setup.

The gastro-intestinal region is described by four compartments: the gastric lumen ($GL$), the small intestinal lumen ($SIL$), the large intestinal lumen ($LIL$), and the gastro-intestinal circulatory system ($GICS$). This last compartment, even if it is an anatomical portion of the gastrointestinal region, will be discussed as an element of a second functional region (*i.e.* cardio-circulatory system) and detailed below. For the sake of clarity, the symbology assigns capital letters to compartment names to avoid confusion with real organ names (though there can be a direct correspondence between an organ and its compartmental schematization, *e.g.*, liver-Liver). The symbology adopts letters for every parameter, with superscripts to

specify the location within the model where the parameter is applied, and subscripts to provide further information about the function/action performed. See the Notation section for further details.

The $GL$, $SIL$, and $LIL$ compartments schematize respectively the stomach and main tracts of the intestine (*i.e.* small and large lumina), which are the sites where drug absorption occurs in case of oral administration (*i.e. PO* from the Latin locution "*per os*", *i.e.* "*by mouth*"). Accordingly, the flow of the oral bolus along the whole digestive system is described by $F^{GL}$, $F^{SIL}$, and $F_E^{LIL}$, which are the material flows and are defined as the concentrations ($C^{GL}(t)$, $C^{SIL}(t)$, and $C^{LIL}(t)$) divided by the corresponding residence times in the lumina ($t^{GL}$, $t^{SIL}$, and $t^{LIL}$), for instance $F^{SIL} = \frac{C^{SIL}}{t^{SIL}}$. Mass transport phenomena, related to drug absorption along the intestinal tracts, can proceed in both directions (*i.e.* from the intestine to the $GICS$ and vice versa) depending mainly on the concentration gradients and being a function of mass transfer coefficients: $j_A^{SIL}$ and $j_A^{LIL}$ (for the absorption from the intestinal lumina); $j_{CA}^{SIL}$ and $j_{CA}^{LIL}$ (for the counter absorption). In general, mass transfer through the barrier of the gastric lumen can be neglected due to the high resistance to diffusion played by the stomach wall coupled to a rather short residence time (*e.g.*, 20-30 min) of the administered drug (usually favored by ingested liquids). Finally, $F_E^{LIL}$ is the elimination term that accounts for the drug expelled via faeces.

A second physiological region describes the drug circulation in the body and is schematized by three compartments. The first one symbolizes the $GICS$ that collects blood channels from the intestine to the liver via the portal vein. This compartment represents an innovation in physiologically-based pharmacokinetic modeling, as it allows to effectively lump very detailed pharmacokinetic models (*e.g.*, the one proposed by Jain *et al.*, (1981)). The introduction of $GICS$ allowed Di Muria *et al.* (2010) to carry out a simpler and more effective model (with 7 compartments, *i.e.* 7 ODEs, and about twenty adaptive parameters), an effort in which several researchers spent a lot of work, with limited results (see for instance Nestorov *et al.*, 1998). Basically, $GICS$ lumps the mesenteric artery (*i.e.* the artery which supplies the gastrointestinal tract), the portal vein (*i.e.* the vein which departs from the gastrointestinal tract towards the liver), and the ensemble of microcirculatory gastrointestinal vessels. This portion of circulatory system behaves differently from the remaining one. In case of enteral administration, the portal vein conveys the drug from the gastrointestinal tract towards the liver, where it experiences the so-called first-pass effect. $Q^{PV}$ is the volumetric flow rate in the portal vein that reaches the liver. Eventually, the drug moves to the remaining part of the circulatory system (here called Plasma) and the other tissues. In case of parenteral administration, the mesenteric artery transports the drug towards the gastrointestinal tract.

It is worth clarifying the relation between blood and plasma, as plasma is the liquid fraction of blood. The mathematical model here proposed refers always to the plasma fraction of blood with further comments on blood composition given in the following sections.

The liver is the metabolic center of the organism. Here a large amount of complex molecules are metabolized. The hepatic clearance ($CL^H$) quantifies the metabolic activity of the liver and is defined as the volume of plasma that is purified from drug molecules in the time unit. When the plasma leaves the liver, it enters the hepatic vein that is part of the systemic circulation. $Q^{HV}$ is the volumetric flow of plasma in the hepatic vein. Through the Plasma compartment, the drug can now reach every organ and tissue of the body. It is worth observing that in case of intravenous administration ($IV$) the drug is injected directly into the Plasma compartment. As aforementioned, the Plasma compartment refers exclusively to the liquid fraction of blood, which is indeed composed of plasma and cells (*e.g.*, erythrocytes, leukocytes, and platelets). Our model considers only the plasma volume as this fraction is the liquid vehicle that makes possible the drug transport throughout the organism. In addition, water is the most prevalent element of plasma (over 91% mass fraction) and has the function of "solvent and suspending medium" (Tortora and Nielsen, 2014). A specific parameter ($R$) is introduced to consider the drug fraction bound to plasma

proteins, which are 7% of plasma. $R$ is specific to every drug molecule and affects deeply the distribution process. According to our understanding, possible interactions of drugs with hematocrit components are negligible and it was not possible to find any evidences/references in literature to justify further this issue. A detailed discussion about $R$ role in the numerical PBPK model is provided in Section 3.3.

The Plasma compartment conveys the drug to the organs and tissues by means of four terms:

(i)     a fraction of plasma ($Q^{PV}$) circulates through the $GICS$ to the liver via the portal vein;

(ii)    a fraction of plasma ($Q^{HA}$) is delivered directly to the liver through the hepatic artery;

(iii)   $j_{P-PT}$ accounts for the transport phenomena from Plasma to Poorly perfused Tissues;

(iv)    $j_{P-HO}$ accounts for the transport phenomena from Plasma to Highly perfused Organs.

In addition, (iii) and (iv) terms have two counterparts that are $j_{PT-P}$ and $j_{HO-P}$ for the counter mass transfer from tissues and organs into plasma.

Besides the hepatic clearance and the faeces, the mPBPK model considers three additional elimination terms that are responsible for the drug metabolism and excretion:

(i)     the direct metabolism of the drug molecules in the plasma with $k_E^P$ being the corresponding coefficient;

(ii)    the kidneys clearance ($CL^K$), which quantifies the drug fraction filtered from plasma by kidneys and excreted with urine;

(iii)   $k_E^T$ accounts for the metabolic reactions that occur in the compartment of Poorly perfused Tissues.

The first two terms belong to Plasma whilst the last one refers to the tissue metabolism. For the sake of accuracy, both terms $CL^H$ and $CL^K$ quantify the total plasma volumetric flow reaching the organs (*i.e.* $Q^H$ and $Q^K$) multiplied by the organ efficiency (*i.e.* $Eff^H$ and $Eff^K$). The quantification of these terms is a compromise between specificity and generality. Indeed, the organ plasma flow rates are individualized, *i.e.* they depend directly on the body features of each patient (as explained in the following). Conversely, the organ efficiencies assume general values that are independent of patient's features (although in presence of patients' clinical data, the efficiency term could also be individualized by knowing organs impairment status). It is worth observing that the kidneys clearance ($CL^K$) applies directly to Plasma and not to the Highly perfused Organs, to which the kidneys belong physiologically. The reason is linked to renal physiology: the functional unit for drug elimination is the nephron, which conveys filtered drug to the bladder in three steps (*i.e.* filtration, tubular secretion, and tubular reabsorption), a detailed definition of kidneys physiology can be found in Bauer (2008), and Tortora and Nielsen (2014). Since filtration occurs directly from blood vessels reaching the nephrons, our model considers this elimination term ($CL^K$) applied to Plasma.

A third physiological region comprises two compartments, (i) Poorly perfused Tissues (PT) and (ii) Highly perfused Organs (HO). These compartments lump the remaining tissues and organs that are not considered individually by the model. This model adopts a perfusion-limited distribution approach, which means that the bottleneck of drug transport from plasma to tissues is mainly due to blood convection with a minor role of biological membrane diffusivity. This classification appeared in previous literature studies and the concept of peripheral compartment with poor drug disposition capability was discussed in Wagner (1993). In particular, the compartment of Poorly perfused Tissues lumps the body elements that are not much perfused by blood. In these organs and tissues the drug transport is somehow hindered (*e.g.*, muscles, skin, heart, bones). The compartment of Highly perfused Organs lumps the organs that are richly perfused by blood (*e.g.*, spleen, lungs, brain, kidneys, sexual organs).

To sum up, the mPBPK model comprises eight compartments that are mathematically described by a system of eight ODEs, which quantify the mass balances across the various compartments. These Equations

(1-8) inherit the formulation of Di Muria *et al.* (2010) but implement the modifications and innovations discussed above, which are based mostly on physiological phenomena. Basically, these are: the addition of Highly perfused Organs; the redefinition of Plasma; the quantification of the drug in the gastrointestinal lumina in terms of concentration rather than total mass; a new formulation for the equation which governs the transit and the absorption across the intestine; the introduction of the fraction of drug bound to plasma proteins, which makes the plasma volume a real physiological quantity. It is worth underlining that the new representation of Plasma allows evaluating the real plasma volume and, as a consequence, determining dynamically the amount of drug present in the blood. Furthermore, the $R$ parameter enables to quantify which fraction of the circulating drug can really distribute in the organism (*i.e.* is bioavailable). Some specific parameters, as $j_{CA}^{SIL}$, $j_{CA}^{LIL}$, and $k_E^T$ allow to keep up the fidelity with the physiological activity of the organism.

$$\frac{dC^{GL}(t)}{dt} = \frac{PO(t)}{V^{GL}} - F^{GL}(t) \tag{1}$$

$$\frac{dC^{SIL}(t)}{dt} = -C^{SIL}(t)j_A^{SIL} + F^{GL}(t)\frac{V^{GL}}{V^{SIL}} - F^{SIL}(t) + C^{GICS}(t)j_{CA}^{SIL}(1-R)\frac{V^{GICS}}{V^{SIL}} \tag{2}$$

$$\frac{dC^{LIL}(t)}{dt} = -C^{LIL}(t)j_A^{LIL} + F^{SIL}(t)\frac{V^{SIL}}{V^{LIL}} - F_E^{LIL}(t) + C^{GICS}(t)j_{CA}^{LIL}(1-R)\frac{V^{GICS}}{V^{LIL}} \tag{3}$$

$$\frac{dC^P(t)}{dt} = -C^P(t)\left( j_{P-PT}(1-R) + j_{P-HO}(1-R) + \frac{Q^{HA}}{V^P} + \frac{Q^{PV}}{V^P} \right) + C^{PT}(t)j_{PT-P}\frac{V^{PT}}{V^P} +$$

$$+C^L(t)\frac{Q^{HV}}{V^P} + C^{HO}(t)j_{HO-P}\frac{V^{HO}}{V^P} - C^P(t)k_E^P(1-R) - C^P(t)\frac{CL^K}{V^P} + \frac{IV(t)}{V^P} \tag{4}$$

$$\frac{dC^{PT}(t)}{dt} = -C^{PT}(t)\left( j_{PT-P} + k_E^T \right) + C^P(t)(1-R)j_{P-PT}\frac{V^P}{V^{PT}} \tag{5}$$

$$\frac{dC^{GICS}(t)}{dt} = -C^{GICS}(t)\left( \frac{Q^{PV}}{V^{GICS}} + j_{CA}^{SIL}(1-R) + j_{CA}^{LIL}(1-R) \right) + C^{SIL}(t)j_A^{SIL}\frac{V^{SIL}}{V^{GICS}} +$$

$$+C^{LIL}(t)j_A^{LIL}\frac{V^{LIL}}{V^{GICS}} + C^P(t)\frac{Q^{PV}}{V^{GICS}} \tag{6}$$

$$\frac{dC^L(t)}{dt} = -C^L(t)\left( \frac{Q^{HV}}{V^L} + \frac{CL^H}{V^L} \right) + C^P(t)\frac{Q^{HA}}{V^L} + C^{GICS}(t)\frac{Q^{PV}}{V^L} \tag{7}$$

$$\frac{dC^{HO}(t)}{dt} = -C^{HO}(t)j_{HO-P} + C^P(t)j_{P-HO}(1-R)\frac{V^P}{V^{HO}} \tag{8}$$

Once solved numerically, the model describes the dynamic concentration profiles of the drug in every compartment (identified by the concentration subscripts in the differential terms). The material flows, which enter and leave the compartments, are described by the ODEs right-hand sides of Equations (1-8). The sign convention assumes that positive flows enter the compartments and negative flows leave them. Mass transport occurs in two main ways: (i) through simple mass transfer, in this case concentration ($C$) multiplies a mass transfer coefficient ($j$); (ii) via blood circulation, in this case ($C$) multiplies a plasma volumetric flow ($Q$). The drug administration (see also Figure 1) can be either oral ($PO$), or intravenous ($IV$). Both terms assess the amount of mass which is administered in the time unit and at a given administration site. Elimination routes are $F_E^{LIL}$, $CL^H$, $CL^K$, $k_E^T$, and $k_E^P$.

In order to quantify the different contributions to drug metabolism and excretion, the following supplemental Equations (9-13) may result useful:

$$\frac{dM_E^{LIL}(t)}{dt} = \frac{C^{LIL}(t)}{t^{LIL}}V^{LIL} \tag{9}$$

$$\frac{dM_E^P(t)}{dt} = C^P(t)(1-R)k_E^P V^P \tag{10}$$

$$\frac{dM_E^T(t)}{dt} = C^T(t)k_E^T V^T \tag{11}$$

$$\frac{dM^H(t)}{dt} = C^L(t)CL^H \tag{12}$$

$$\frac{dM^K(t)}{dt} = C^P(t)CL^K \tag{13}$$

Here $M$ is the total amount of drug [ng] that is eliminated through different pathways. Equation (9) refers to the amount of drug eliminated with the faeces. Equations (10) and (11) refer to drug metabolized in plasma and tissues respectively. Finally, Equations (12) and (13) refer to drug removed by liver and kidneys respectively. It is worth observing that these equations do not take part to the definition of the ODEs system, but are only used to quantify ancillary information.

For the sake of rigorousness, the intestinal lumen should be modeled as a longitudinal duct rather than a perfectly mixed bowl. By adopting a similarity with industrial equipment, the intestinal lumen resembles more a plug flow reactor (*i.e.* PFR) than a continuously stirred tank reactor (*i.e.* CSTR). Consequently, Equations (2-3), which in their present formulation describe the dynamics of perfectly stirred compartments, should be modified to comply with the diffusion of the oral bolus along those lumina. This model improvement would introduce partial differential equations (PDE) as two independent variables would be needed to describe the time and space evolution. A viable simplifying approach to PDE solution consists in discretizing spatially the PDE in a series of perfectly mixed sub-compartments (which match asymptotically the PFR hypothesis). By doing so, each PDE becomes a set of ODEs, whose number depends on a suitable compromise between discretization detail and CPU efficiency. This paper keeps the formulation of Equations (2-3) at the maximum degree of simplification (*i.e.* in the original ODE formulation) as the proposed case study deals with an intravenous drug administration that does not directly involve the gastro-intestinal compartments (see also Section 3.2 for further details). Conversely, Abbiati *et al.* (2015a) implemented the mathematical discretization of the PFR lumen into a series of CSTR discrete sub-compartments with the PBPK simulation of sorafenib, an antitumoral drug administered orally (via tablets).

The total number of parameters in Equations (1-8) is 28. Table 1 classifies them into three main classes: (i) individualized, (ii) assigned, and (iii) unknown parameters. These three classes will be discussed in the following sections.

Table 1 - Model parameters.

| Symbol | Units | Description | Type |
|---|---|---|---|
| $Q^{HA}$ | ml/min | Hepatic Artery volumetric flow (of plasma) | Individualized |
| $Q^{HV}$ | ml/min | Hepatic Vein volumetric flow (of plasma) | Individualized |
| $Q^K$ | ml/min | Volumetric flow of plasma to Kidneys | Individualized |
| $Q^{PV}$ | ml/min | Portal Vein volumetric flow (of plasma) | Individualized |
| $V^{GICS}$ | cm$^3$ | $GICS$ compartment volume | Individualized |
| $V^{GL}$ | cm$^3$ | $GL$ compartment volume | Individualized |
| $V^{HO}$ | cm$^3$ | Highly perfused Organs compartment volume | Individualized |
| $V^L$ | cm$^3$ | Liver compartment volume | Individualized |
| $V^{LIL}$ | cm$^3$ | $LIL$ compartment volume | Individualized |
| $V^P$ | ml | Plasma compartment volume | Individualized |
| $V^{PT}$ | cm$^3$ | Poorly perfused Tissues compartment volume | Individualized |

| $V^{SIL}$ | cm$^3$ | $SIL$ compartment volume | Individualized |
|---|---|---|---|
| $R$ | - | Drug fraction bound to plasma proteins | Assigned |
| $t^{GL}$ | min | $GL$ residence time | Assigned |
| $t^{LIL}$ | min | $LIL$ residence time | Assigned |
| $t^{SIL}$ | min | $SIL$ residence time | Assigned |
| $Eff^H$ | - | Hepatic efficiency of elimination | Unknown parameter |
| $Eff^K$ | - | Kidneys efficiency of elimination | Unknown parameter |
| $j_A^{LIL}$ | min$^{-1}$ | $LIL$ to $GICS$ mass transfer coefficient | Unknown parameter |
| $j_A^{SIL}$ | min$^{-1}$ | $SIL$ to $GICS$ mass transfer coefficient | Unknown parameter |
| $j_{CA}^{LIL}$ | min$^{-1}$ | $GICS$ to $LIL$ mass transfer coefficient | Unknown parameter |
| $j_{CA}^{SIL}$ | min$^{-1}$ | $GICS$ to $SIL$ mass transfer coefficient | Unknown parameter |
| $k_E^P$ | min$^{-1}$ | Plasma Elimination kinetic rate constant | Unknown parameter |
| $k_E^T$ | min$^{-1}$ | Tissues Elimination kinetic rate constant | Unknown parameter |
| $j_{HO-P}$ | min$^{-1}$ | Highly perfused Organs to Plasma mass transfer coefficient | Unknown parameter |
| $j_{P-HO}$ | min$^{-1}$ | Plasma to Highly perfused Organs mass transfer coefficient | Unknown parameter |
| $j_{P-PT}$ | min$^{-1}$ | Plasma to Poorly perfused Tissues mass transfer coefficient | Unknown parameter |
| $j_{PT-P}$ | min$^{-1}$ | Poorly perfused Tissues to Plasma mass transfer coefficient | Unknown parameter |

## 2.2 Model analysis

The PBPK model is a system of ordinary differential equations in the independent variable time ($t$). Dependent variables are the concentrations ($C$) in every compartment, so the model output is the dynamic evolution of these concentrations. In its complete formulation, the model requires eight equations (*i.e.* Equations 1-8), each of them describing a mass balance related to drug disposition in a specific compartment. Some auxiliary equations are used to derive useful information (*i.e.* Equations 9–13), but those are not part of the intrinsic model structure. The capability of the model to describe the simulated PK is intrinsically related to the parameters assignment. The 28 parameters of the model are categorized into three main groups (see Table 1). Individualized parameters depend on patient characteristics, hence the name "Individualized", and are calculated with literature correlations. "Assigned" parameters are constant for every patient. Remaining parameters are "Unknown" and determined via a regression procedure of pharmacokinetic experimental data. Sections 2.4 and 3.3 provide further details on the numerical calculation of these parameters. Equations 14-22 are explicit formula (*i.e.* they do not require to be solved but just calculated) used to determine the "Individualized" parameters.

The mPBPK model is a convenient tool for several applications because it generates PK predictions only in some selected compartments, which are usually of interest for physicians. Further details are provided as lumped outputs (as in case of drug concentrations in the lumped compartments). At the same time, the model preserves a description of the most important ADME processes, as drug distribution, metabolism, and elimination are acknowledged. In our opinion this provides simplicity to the PK modeling as it requires an ODE system of small dimensions and few equation parameters, respect to more complex full-PBPK models in the literature.

Finally, the proposed mPBPK model can be further reduced according to the administration route (*e.g.*, endovenous administration) as shown in Section 3.2. Indeed, as an endovenous injection administers the drug directly in the blood, it is then possible to neglect the gastro-intestinal region because the intestinal drug absorption does not occur. This allows reducing the number of involved equations (*i.e.* $GL$, $SIL$, $LIL$ equations are neglected), and condensing the number of model parameters and dependent variables (*i.e.* drug concentration in $GL$, $SIL$, $LIL$ compartments).

## 2.3   Modeling approach

The following two sections discuss the methodology adopted to customize the mPBPK model described in Equations (1-8) to a specific case-study, assign the constants, and estimate the unknown parameters that characterize its structure.

This work presents some further steps for the complexity reduction of the mPBPK model that are based on reducing the number of compartments, which have to be solved numerically, and on eliminating the material flows that assume a negligible role as a function of the specific drug and its administration route. To proceed with this activity, an accurate literature survey allows understanding in depth the key points of the drug biodistribution. Once the mPBPK structure is fully defined, the attention focuses on assigning the parameters whose values are available in the literature. By doing so, the number of unknown parameters that must be identified gets reduced significantly (as reported in Table 4). This makes the nonlinear regression procedure, which is used to evaluate the unknown parameters, more robust and efficient.

## 2.4   Evaluation of the model parameters

Different approaches are adopted to calculate, assign, and fit the model parameters according to the abovementioned three classes. Individualized parameters are estimated via specific correlations available in the literature (Brown *et al.*, 1997), which depend on two basic patient features: gender and body mass. This means that individualized parameters are characteristic of each patient and in this sense they are personal. Indeed, it is rather evident that the dimension and gender of the patient can play a significant role in the administered dose and its dynamic evolution in the body. The ultimate goal is to refine those correlations further via the availability of more advanced equations and a few more patient's data (*e.g.,* age, cardiac pressure, race, specific organ failures) and to increase the number of parameters which can be individualized rather than assigned or assumed as unknown parameters.

The parameters belonging to the "assigned" class cannot be individualized because of the lack of patient-dependent correlations in the literature. However, it is still possible to either determine these parameters experimentally or find proper values in the literature. For this reason they are given a constant value, which is patient independent.

Finally, the unknown parameters (*e.g.,* the mass transfer coefficients $j_{PT-P}$ or $j_{P-PT}$) do not have a direct correspondence with a physiological property and therefore need to be determined via a mathematical correlation/formula. Consequently, they can be estimated by a nonlinear regression routine that minimizes the sum of the squared errors between the experimental data of drug concentration in the blood and the model data. In general, the regression routine could use all the experimental data of drug concentrations in the different organs and tissues as modelled by Equations (1-8). However, this is hardly possible, as far as human patients are involved in the experimental activity, since the only drug concentration that can be feasibly measured is the concentration in the blood. Concentration measures in tissues are possible for humans, via biopsies, but these techniques are invasive and can evaluate only small fractions of tissues. In case of experimental tests, the animals (*e.g.,* rats, mice) can be sacrificed periodically during the drug's ADME pathways. This allows measuring the drug concentration at given time intervals in different organs and tissues. As the sacrificed animals are no more available after the measure, then different individuals must be used at every sampling time. This point sets a consistency problem of body features among different individuals. Actually, in case of rats and mice, the strict selection criteria adopted by guinea-pig suppliers allow assessing a somewhat aprioristic consistency of individuals whose body features can be considered constant and independent of each single subject.

The parametric nonlinear regression is based on a constrained optimization algorithm that allows keeping the unknown parameters (*i.e.* the adaptive parameters to be identified) inside a feasible region, which is

defined according to sound hypotheses based on the physics of the modeled system (*e.g.,* mass transfer coefficients have to be positive; organ efficiencies belong to the 0,…1 interval).

# 3   Case study

In order to validate the proposed model and verify its reliability, a case-study simulates the bolus endovenous injection of different doses (2, 5, 15, 30 µg/kg) of remifentanil in mixed groups of human patients. The simulation results are then compared to the experimental PK data of Westmoreland *et al.*, (1993).

## 3.1   Remifentanil

Remifentanil is an analgesic drug belonging to the fentanyl family. It explicates its pharmacological effect by acting as a direct agonist on µ-opioid receptors. In terms of pharmacodynamic effects, it produces analgesia, respiratory depression, hypotension, and bradycardia (Egan, 2000). Remifentanil may cause muscular rigidity, nausea, and other side effects (Duthie, 1998). The property which makes remifentanil particularly suitable for several applications in surgery, respect to other analgesics, is its short half-life time in the organism. This is due to the rapid hydrolysis of the ester group in blood and tissues by non-specific esterases to form a carboxylic acid metabolite, whose analgesic effect (estimated to be 1/300-1/1000 of the remifentanil one) is negligible (Westmoreland *et al.*, 1993). Specific studies demonstrated that the contribution of kidneys and liver to drug elimination is limited (Pitsiu *et al.*, 2004; Dershwitz *et al.*, 1996). Remifentanil distribution to the brain is not affected by the blood-brain barrier in a way that it rapidly equilibrates at the plasma/effect-site interface (Beers and Camporesi, 2004). The drug fraction bound to plasma proteins is estimated to be 70% (Egan *et al.*, 1998). The rapid metabolism of remifentanil favors its elimination from the organism together with the disappearance of the analgesic effect.

## 3.2   Reduction of the model complexity

The tailored reduction of the mPBPK model requires considering in detail the drug properties. Remifentanil is administered by endovenous infusion. For this reason, the gastrointestinal tract compartments can be neglected by assuming secondary the drug counterdiffusion from the gastrointestinal circulatory system to the gastrointestinal lumina. Since remifentanil is a lipophilic molecule, the diffusion process across the cell membrane is facilitated and this promotes the drug distribution. Remifentanil is known to be almost fully catabolized by esterases in plasma and tissues (*i.e.* muscles and fat, which are poorly perfused tissues according to the proposed model). This allows assigning more importance to the $k_E^P$ and $k_E^T$ terms rather than other minor routes of elimination (*i.e.* $CL^H$ and $CL^K$). Figure 2 shows the structure of the reduced mPBPK model for the $IV$ administration.

This reduced mPBPK model is easier to handle as it features just 5 ODEs instead of the original 8 ones (as the gastric lumen, and small and large intestinal lumina are neglected). In addition, the adaptive parameters (*i.e.* the unknown parameters of the nonlinear regression) are only 8 instead of the original 12. The individualized parameters are further reduced because the volumes of the gastrointestinal region are no more required. Conversely, the assigned parameters are not affected by this simplification.
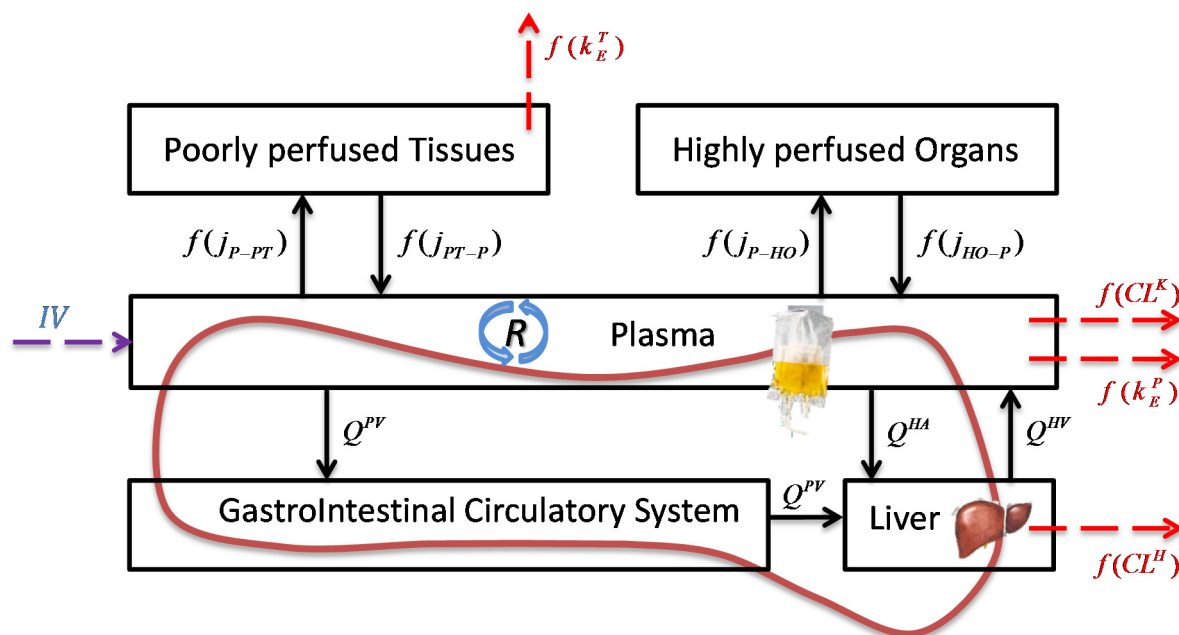
Figure 2: Reduced mPBPK model structure for $IV$ administration route.

## 3.3 Parameters assessment

Before simulating the pharmacokinetics, it is necessary to assign/determine the parameter values. Both the "individualized" and "assigned" parameters are evaluated by means of suitable correlations and experimental/literature data, as introduced in Section 2.4.

Firstly, it is necessary to determine the cardiac output ($CO$) of the patients from literature correlations (Equations 14-15). Secondly, the blood flow rates ($B^X$ with $X = PV, HA, HV, K$) to specific organs can be assessed as a fraction of $CO$ (Equations 16-19). Eventually, Equation 20 converts $B^X$ into plasma flow rates ($Q^X$) as they are simply a fraction of blood flow rates (indeed, plasma is 54% of blood volume). For the sake of clarity, plasma flow rates ($Q^X$) are the parameters introduced in the model equations (Equations 1-8). The quantification of total $CO$ relies on two alternative correlations that depend on the availability of data respect to different body features. When the body surface area ($BSA$) is available, then the following correlation applies (Cowles *et al.*, 1971):

$$CO = 3.5\,BSA \qquad (14)$$

In case of body mass ($BM$), the following $CO$ formula holds (Linsted and Schaeffer, 2002):

$$CO = 0.084\,BM \qquad (15)$$

The cardiac output ($CO$) contributes at different levels to the blood flow rates ($B^X$ of Equations 16-19) with slightly different correlations available for males and females (Williams and Leggett, 1989). In case of mixed groups of patients, averaged values are used (Williams and Leggett, 1989):

$$B^{PV} = 0.20\,CO \qquad (16)$$

$$B^{HA} = 0.06\,CO \qquad (17)$$

$$B^{HV} = 0.26\,CO \qquad (18)$$

$$B^{K} = 0.18\,CO \qquad (19)$$

Since model equations refer to plasma flowrates ($Q^X$), translation of $B^X$ terms into $Q^X$ is possible by applying Equation 20, where 0.54 is the plasma fraction in blood:

$$Q^X = 0.54\,B^X \qquad (20)$$

Equation (21) allows evaluating the compartment volumes that depend on the patient's body mass ($BM$), the organ/tissue body mass fraction ($w_{BM,i}$), and organs/tissues density ($\rho_i$):

$$V = \sum_i \frac{BM\, w_{BM,i}}{\rho_i} \tag{21}$$

where index $i$ lumps the following organs and tissues:

  (i)   fat, bones, heart, skin, muscles (*i.e.* Poorly perfused Tissues);
  (ii)  brain, kidneys, spleen (*i.e.* Highly perfused Organs);
  (iii) liver;
  (iv)  gastro intestinal circulatory system;
  (v)   plasma.

It is worth observing that lungs are not included in the (ii) compartment because of their peculiar nature. Being extremely rich of blood and with a very low density when expanded, the lungs are quite challenging if a reliable value of their actual volume has to be assessed. In addition, the sexual organs were intentionally ignored as coherent literature data are not available and their volume can be assumed negligible respect to other organs. Table 2 reports the body mass fraction and density values of organs and tissues.

Table 2 - Organs/Tissues characteristic data (Brown *et al.*, 1997).

| Organ/Tissue | $BM$ fraction ($w_{BM}$) [-] | Density ($\rho$) [g/ml] |
|---|---|---|
| Blood | 0.079 | 1.06* |
| Bones | 0.143 | 1.6** |
| Brain | 0.02 | 1.035 |
| Fat | 0.214 | 0.916* |
| GICS | 0.0001766*** | 1* |
| Heart | 0.005 | 1.03 |
| Kidneys | 0.004 | 1.05 |
| Liver | 0.026 | 1* |
| Muscles | 0.4 | 1.041 |
| Skin | 0.037 | 1.3** |
| Spleen | 0.00026 | 1.05 |

  * Value taken from other sources.
  ** Average value.
  *** As far as the determination of the $GICS$ volume is concerned, as no correlations are available in the literature, a new formula is herein proposed. Based on an estimation of the volume of the portal vein (diameter data were found in Weinreb *et al.*, 1982, while length data were found in Ongoiba *et al.*, 2003), which is the main constituent of the $GICS$ compartment, and referring to an 80 kg $BM$ patient, the body mass fraction coefficient can be calculated as follows:

   • portal vein geometry assumed cylindrical;
   • portal vein average length =5.8 cm;
   • portal vein average diameter = 1.1 cm.

  Since the entire $GICS$ is not limited to the portal vein itself, but includes all the blood vessels rooting the gastrointestinal tract, those values were opportunely overestimated by 35%, and rounded to 8 cm length and 1.5 cm diameter (ρ=1).

$$w_{BM,GICS} = \frac{V^{PV}\rho}{1000\,BM} = 0.0001766 \tag{22}$$

Table 3 reports the compartment volumes and blood flow rates estimated by applying these formulas to the patient groups of Westmorland *et al.* (1993).

Table 3 - Individualized parameter values.

| Parameters | Group 1 [2 µg/kg] | Group 2 [5 µg/kg] | Group 3 [15 µg/kg] | Group 4 [30 µg/kg] | Units |
|---|---|---|---|---|---|
| $V^{PT}$ | 60059.5 | 58726.5 | 56764 | 59356 | $cm^3$ |
| $V^{HO}$ | 1899.3 | 1857.1 | 1795.1 | 1877 | $cm^3$ |
| $V^P *$ | 3263.9 | 3191.5 | 3084.8 | 3225.7 | Ml |
| $V^L$ | 2108.6 | 2061.8 | 1992.9 | 2083.9 | $cm^3$ |
| $V^{GICS}$ | 14.3 | 14 | 13.5 | 14.2 | $cm^3$ |
| $Q^{PV}$ | 735.7 | 719.4 | 695.4 | 727.1 | ml/min |
| $Q^{HA}$ | 220.7 | 215.8 | 208.6 | 218.1 | ml/min |
| $Q^{HV}$ | 956.4 | 935.3 | 904 | 945.2 | ml/min |
| $Q^K$ | 662.2 | 647.5 | 625.8 | 654.4 | ml/min |

\* Plasma volume is equal to 54% of blood volume.

The only parameter known with sufficient accuracy from the literature and that can be assumed constant for each patient is the fraction of remifentanil bound to plasma proteins that is 70%, as detailed in Section 3.1. Accordingly, $R = 0.7$.

The remaining parameters, classified as "unknown parameters" are determined with a nonlinear regression procedure as discussed in Section 2.4 based on the experimental data of Egan *et al.* (1993). In that study, the remifentanil was administered via an endovenous infusion of 20 min at five different doses to ten healthy male volunteers.

The mPBPK model, in its reduced version (see also Figure 2), was applied to simulate these experimental data starting from initial values of the unknown parameters assigned according to sound hypotheses. A multidimensional optimization algorithm minimized the distance between the model predictions and experimental data. The optimal set of unknown parameters (*i.e.* the solution vector of the minimization algorithm) can then be assumed known and constant for all the forthcoming simulations of remifentanil administration in human patients (see Table 4).

Table 4 - Optimal values for the unknown parameters for remifentanil administration in human patients.

| Parameters | Optimized Values | Units | Lower Bounds | Upper Bounds |
|---|---|---|---|---|
| $Eff^H$ | 0.144 | - | 0.1 | 0.3 |
| $Eff^K$ | 0.394 | - | 0.1 | 0.7 |
| $k_E^P$ | 1.732 | $min^{-1}$ | 0 | 3 |
| $k_E^T$ | 0.063 | $min^{-1}$ | 0 | 3 |
| $j_{HO-P}$ | 0.044 | $min^{-1}$ | 0 | 2 |
| $j_{P-HO}$ | 0.662 | $min^{-1}$ | 0 | 2 |
| $j_{P-PT}$ | 0.479 | $min^{-1}$ | 0 | 1 |
| $j_{PT-P}$ | 0.279 | $min^{-1}$ | 0 | 1 |

Figure 3 shows the model simulations obtained with the optimal values of the unknown parameters (determined after the fitting procedure of the experimental data available in Egan *et al.*, 1993).
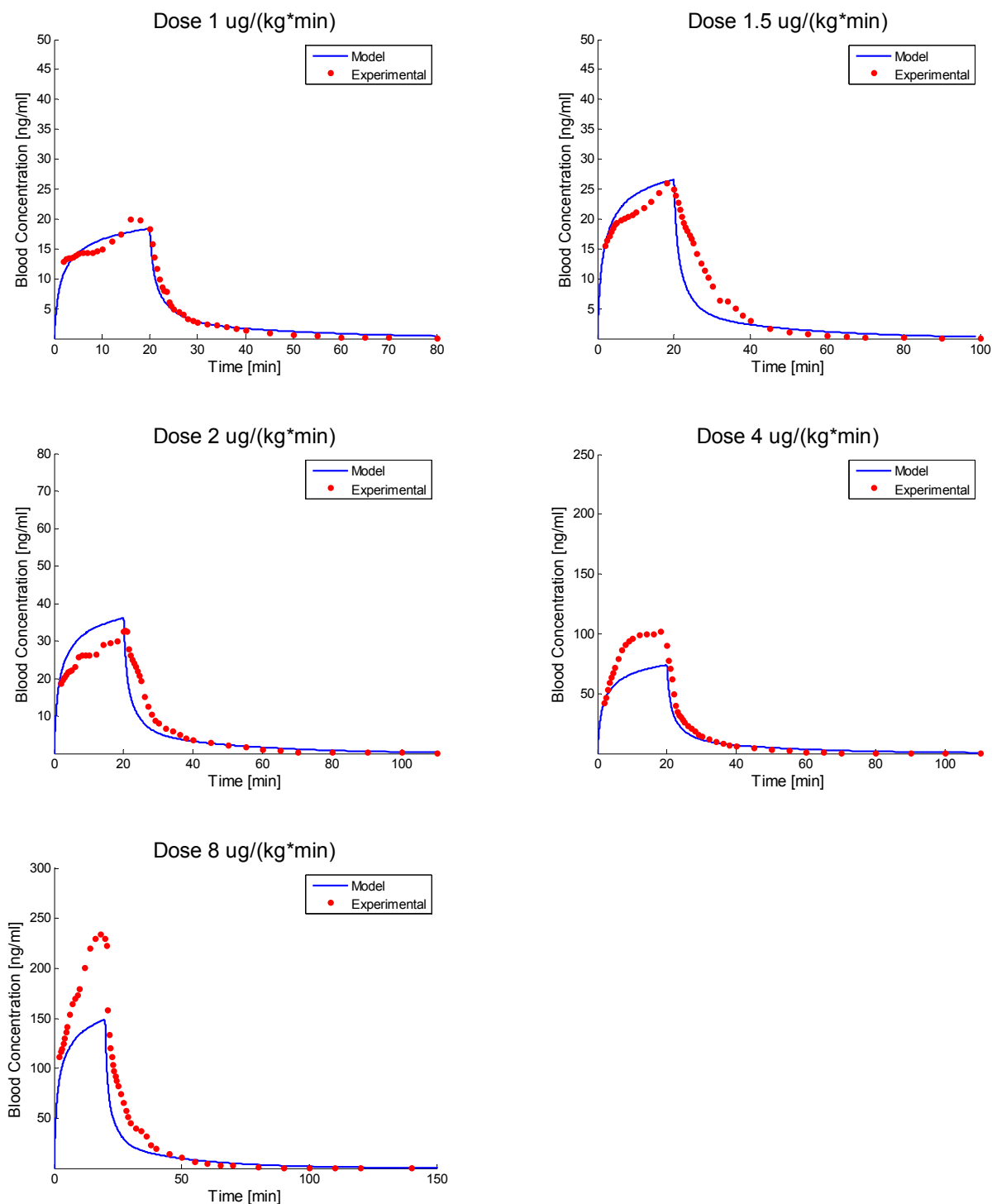
Figure 3: Comparison between the mPBPK model (solid blue lines) and experimental (red marks) data used for the identification of the unknown parameters by the regression procedure. Experimental points (Egan *et al.*, 1993) are single measures of blood concentration at multiple times for individual patients and, as a consequence, no error bars are available.

The regression procedure used all the available data (from ten patients) reported by Egan and coauthors, while for the sake of space just one patient model simulation for each dose is shown in Figure 3. Egan's study involved only healthy adult males in a narrow age range (18-40 y), within 15% of their ideal body weight and with no previous serious diseases. Despite this accurate selection, the individual PK responses revealed dramatic variability. For instance, Figure 4 shows the PK responses of two patients who received

the same remifentanil dose. It is possible to observe the significant differences in both experimental $C_{MAX}$ and $AUC$ values.
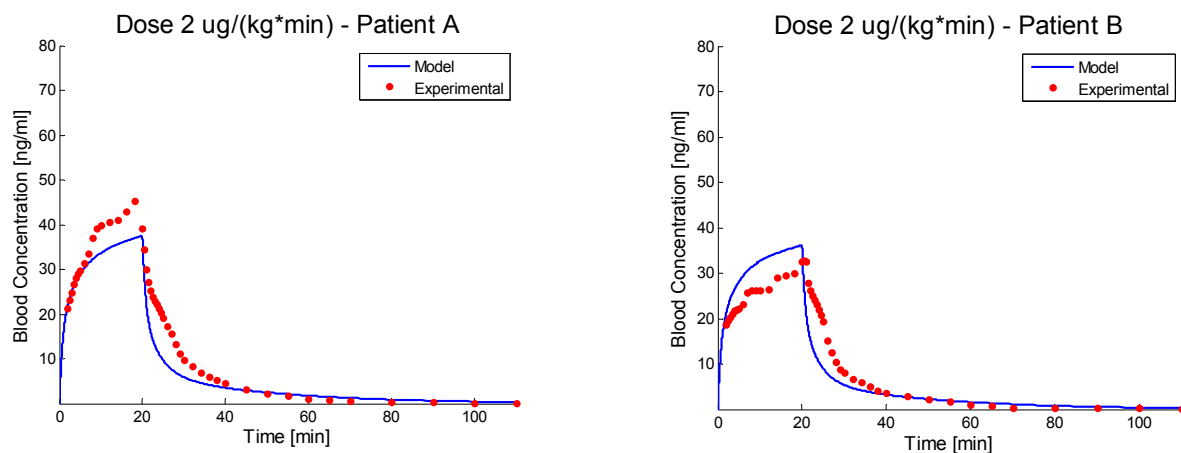


Figure 4: Pharmacokinetic response of two adult male patients to a 20-min administration of 2 µg/kg/min (Egan *et al.*, 1993).

In order to clarify how the whole procedure works, Figure 5 reports a diagram that describes the different blocks and operations commented in Section 3.
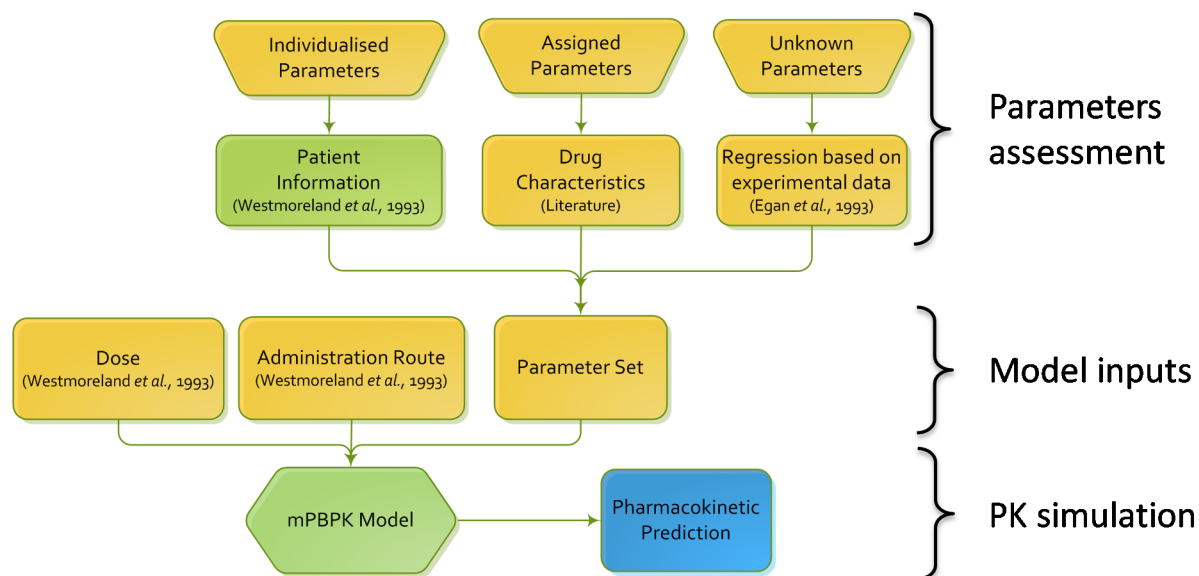


Figure 5: Conceptual organization of the mPBPK model applied to the remifentanil case study.

# 4  Results and Discussion

The model validation is performed by simulating the remifentanil bolus injection according to the experimental setup described in Westmoreland *et al.* (1993). That paper reports the experiments run on 24 patients split into four groups. Each group comprised 6 patients (3 males and 3 females) and received a different dose. Table 5 provides group details about body mass of patients as averaged values.

Table 5 - Patients demographics as reported in Westmoreland *et al.* (1993). Every dose was adminstered to a separate group of six patients (3 males and 3 females), reported quantities are averaged values with SD in parentheses.

| Dose | Remifentanil dose [µg/kg] | | | | | | | |
|---|---|---|---|---|---|---|---|---|
| | 2 | | 5 | | 15 | | 30 | |
| Gender | Male | Female | Male | Female | Male | Female | Male | Female |
| Age [y] | 42.3 (6.4) | 42.3 (6.7) | 39 (14.7) | 37.3 (1.2) | 22.3 (3.8) | 40.7 (6.1) | 52 (8) | 39.7 (10.8) |
| Weight [kg] | 98.6 (9) | 63.6 (7.7) | 91.3 (7.5) | 67.1 (12.9) | 81.7 (9.8) | 71.6 (7) | 92.6 (12.4) | 67.7 (15.5) |

Figure 6 compares the simulated PK curves (solid blue lines) with the experimental data (dashed red lines, with population central value and SD distribution) and allows assessing the reliability of the model. Intentionally, the ordinate axes are not logarithmic (as opposed to most diagrams available in the literature) to avoid any flattening of displayed results and increase the evidence of possible discrepancies (which are practically absent in the obtained diagrams).
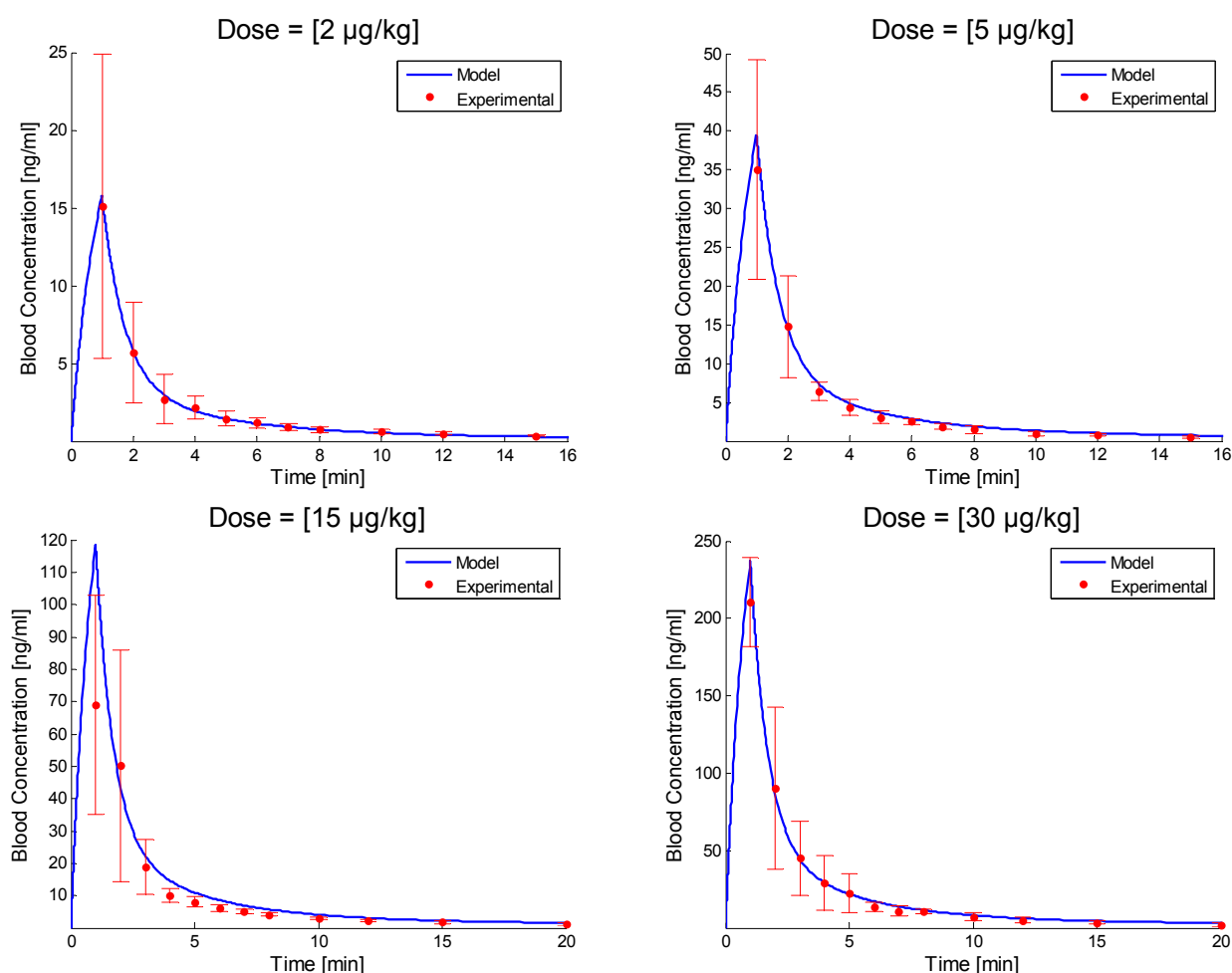


Figure 6: Comparison between mPBPK model (solid blue lines) and experimental (red marks + SD bars) data for remifentanil administration.

The mPBPK model herein presented results suitable to accurately describe the PK behavior of remifentanil in groups of mixed patients and for different injected doses. It is worth highlighting the precision achieved in the simulation of peak concentration ($C_{MAX}$), which is a key PK parameter. In three out of four simulations (*i.e.* 2, 5, and 30 µg/kg doses) the $C_{MAX}$ value is within 13% of the experimental one. Globally,

the simulated curves are rather close to the central values of the experimental distributions and belong to the standard deviation bands for the large majority of the experimental points right after the $C_{MAX}$, which are the most significant ones as in this concentration range the drug exploits its pharmacological effect. Another interesting comparison between the predicted curves and experimental data is the difference in the so called area-under-the curve ($AUC$). Indeed, the $AUC$ plays a primary role in the assessment of both consistency and effectiveness of pharmacokinetics.

Similar values of $C_{MAX}$ and $AUC$ are reliable indexes of a substantial similarity between modeled and experimental concentration profiles. Interestingly, three out of four predictions reveal a relative difference between the $AUC$ values that is below 10% (see also Table 6).

Table 6 - $AUC$ and $C_{MAX}$ comparison between model predictions and experimental data.

| | Group 1 [2 µg/kg] | Group 2 [5 µg/kg] | Group 3 [15 µg/kg] | Group 4 [30 µg/kg] |
|---|---|---|---|---|
| **Δ $AUC$ %** | 9.3 | 7.5 | 30.4 | 5.9 |
| **Δ $C_{MAX}$ %** | 4.5 | 12.8 | 71.7 | 12.9 |

By analyzing these results, it is understandable the difficulty to deal with the inter-individual variability, as can be observed in Figure 7 where the injected dose is compared to the peak blood concentration ($C_{MAX}$) for both model and experimental data. Figure 7 shows a pretty evident linear correlation between the injected dose and the peak concentration in blood. This correlation is lost at the third experimental value (*i.e.* group 3 with an injected dose of 15 µg/kg). Besides the inter-individual variability, the outlier of group 3 suggests also a possible gross error in the experimental measurements or some missing data/details about the patients of that group as per the article of Westmoreland *et al.* (1993).
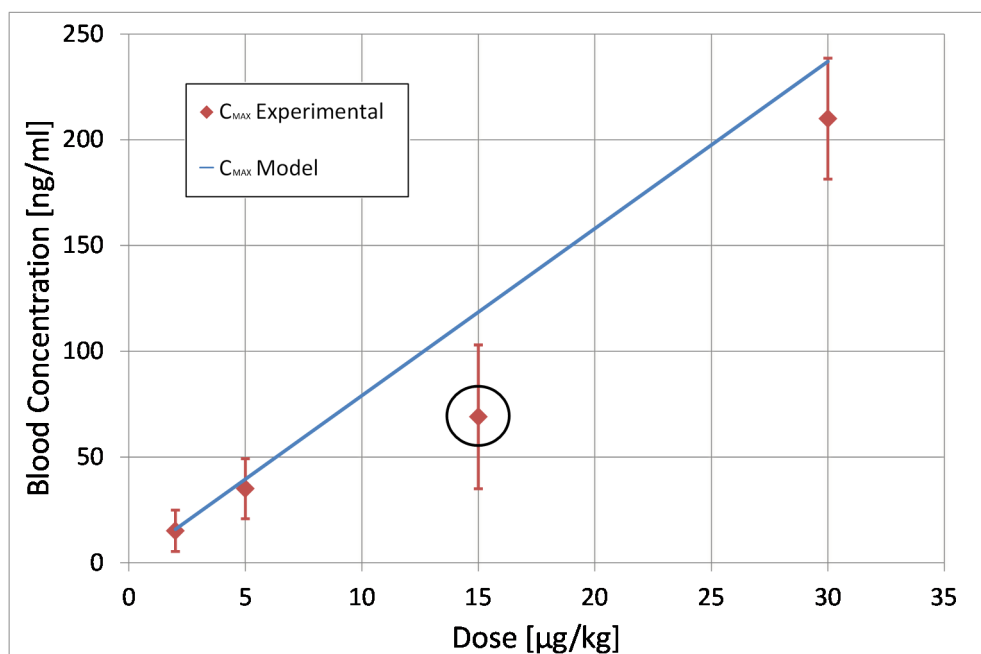


Figure 7: Comparison between model (solid line) and experimental data (diamonds). The black circle highlights the experimental value of $C_{MAX}$ for an injected dose of 15 µg/kg and suggests that it is probably an outlier.

Besides the classical PK data of drug concentration in plasma, the application of a model based on the human physiology provides information on the biodistribution of active principles in specific organs. An organ, which plays a major role in determining the fate of drug kinetics, is indeed the liver. Figure 8

compares the concentration profile in Liver (blue dashed-and-dotted line) with the ones of Poorly perfused Tissues (black solid line) and Highly perfused Organs (red dashed line).
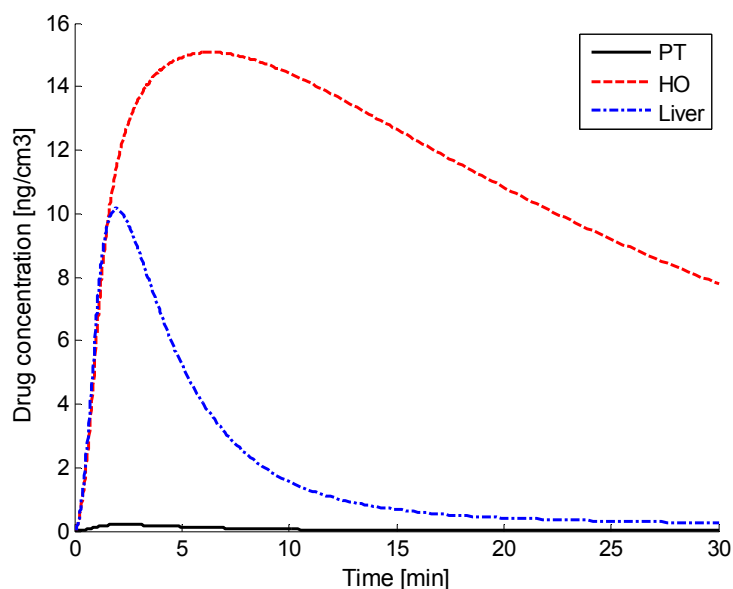


Figure 8: Simulation of drug concentration profiles in the compartments of Poorly perfused Tissues ($PT$), Highly perfused Organs ($HO$), and Liver, for a 2 µg/kg remifentanil dose.
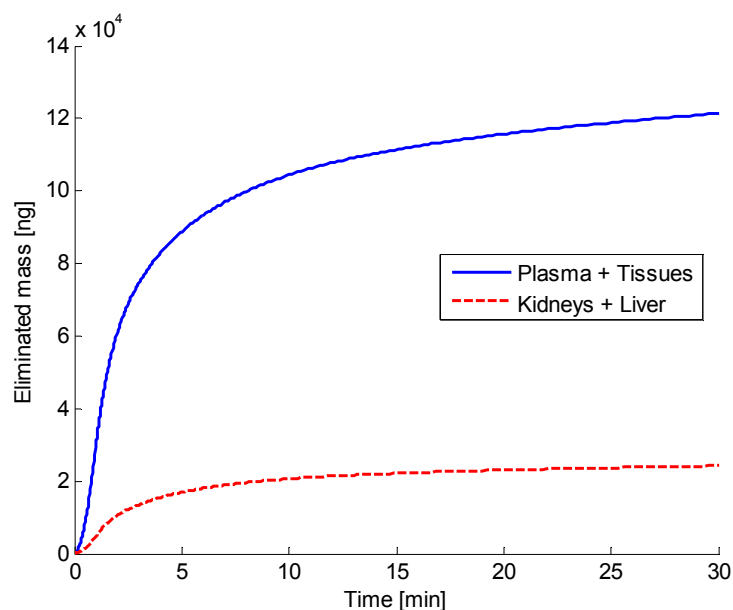


Figure 9: Contribution to drug elimination by kidneys ($CL^K$) and hepatic ($CL^H$) clearance respect to Plasma ($k_E^P$) and ($k_E^T$) tissues metabolism, for a 2 µg/kg remifentanil dose.

The compartment of Highly perfused Organs shows the higher peak of drug concentration ($C_{MAX}^{HO} = 15.07$ ng/cm³, $t_{MAX}^{HO} = 6.37$ min) respect to Liver and Poorly perfused Tissues. This value is respectively 1.48 and 74.3 times higher than the $C_{MAX}$ values reached in Liver and in Poorly perfused Tissues (at $t_{MAX}^{Liver} = 1.96$ min and $t_{MAX}^{PT} = 2.24$ min).

With reference to drug metabolism, the mPBPK model has to reproduce correctly not only the total drug catabolization, but also to meet the contributions of each metabolic pathway. The contribution to drug

excretion by kidneys and hepatic clearances ($CL^K + CL^H$) is about 19.6% respect to the contribution by plasma and tissues biotransformation ($k_E^P + k_E^T$) for all the four groups of patients (see also Figure 9). This confirms the major role played by plasma and tissues catabolism as suggested by experimental evidence.

# 5   Conclusions

This article proposed an mPBPK model designed to provide a general description of the mammalian and specifically of human anatomical/physiological structure. The mPBPK model was devised to preserve the easiness of use. This simplicity does not only deal with the mathematical structure of the ODE system, but also focuses on the parameters that at different levels describe the anatomical and physiological features of the body under study. As the results indicate, the mPBPK model represents a valid alternative to more complex and detailed models (*e.g.*, Jain *et al.*, 1981) that are based on a large number of compartments and physiological parameters, which are difficult (if not impossible) to either measure or find in the literature. From the limitations of those detailed models arose the idea of lumping the tissues and organs whose drug concentration is neither explicitly available nor absolutely necessary. Actually, these organs are simply sites of distribution for the drug. For this reason, the estimation of an averaged PK profile is more than acceptable. By doing so, the number of model parameters is significantly reduced with respect to full-PBPK models such as the one originally proposed by Jain *et al.*, 1981. The overall reduction of model parameters applies also to the unknown ones that are identified by a regression procedure. In this case, the reduction in the number of unknown parameters not only benefits the optimization algorithm, in terms of computation time, but also enhances the robustness of the numerical procedure.

Whenever possible, the parameters of the mPBPK model are either individualized or set as constants based on values found in the literature. Only when a parameter cannot be assigned a value (according to these methodologies) it is then identified with a regression procedure.

The personalization feature proposed in this article is an important point of the discussion as it introduces the concept of adaptation of the PBPK/mPBPK modeling to the specific patient features. The role played by gender, mass, height, age, race, and health history of the patient is of paramount importance in determining the dynamic ADME phenomena that regulate the pharmacokinetics of the administered drug. On one hand, the availability of a robust, efficient, and reliable mPBPK model allows the forecasting of drug dynamics in the patient body, once the prescription has been assigned. On the other hand, the mPBPK model allows solving the so-called "inverse problem", which consists in determining the personal prescription that should be administered to better follow the optimal pharmacokinetic trajectory. Specifically, we are referring to the progressive and pervasive addressing of medical science towards the supply of dedicated products and services tailored to single patients (Laínez-Aguirre *et al.*, 2011; Morse *et al.*, 2015).

As far as the model structure is concerned, the introduction of the new compartment named "Highly perfused Organs", which was formerly merged to Plasma (Di Muria *et al.*, 2010), proved advantageous for two reasons. Firstly, the availability of two compartments dedicated to either Highly perfused Organs or Poorly perfused Tissues introduced flexibility in the model and went in the direction of better interpreting the body features and its physiology. Secondly, the assumption of considering Plasma as a dedicated and standalone compartment increased both the reliability and precision of the model, which was primarily designed to reproduce the drug dynamics in the circulatory system.

Another important feature of the proposed mPBPK model is $R$, which is the fraction of drug bound to plasma proteins. This parameter takes part effectively to the mass transfer phenomena across the cellular membrane. The evaluation of the effective fraction of drug that produces the pharmacological effect is a

goal of PK studies as it affects the initial dose assessment. In perspective, it is also a key parameter for the pharmacodynamic modeling, which describes quantitatively the pharmacologic effect produced by a certain drug concentration on a specific action site. Finally, the combined actions of considering the real plasma volume to quantify the drug concentration and the introduction of $R$ to account for protein binding, guarantee a higher precision and a realistic dynamic assessment of the drug bioavailability in Plasma.

Results from Section 4 confirm the capability of the model to make predictions with reasonable accuracy. The proposed model is rather flexible as concentration profiles can be calculated with a good level of accuracy for different doses and with different infusion methods (*i.e.* bolus respect to continuous infusion). This feature is quite important because the model should work in a large range of possible doses.

Table 6 is also an indicator to better appreciate the quality of PK predictions as FDA (1997) established different levels for *in vivo/in vitro* correlations (IVIVC), where level-A is the highest and guarantees a point-to-point correspondence between predicted and observed values. In order to meet this requirement the Prediction Error % (*i.e.* 100·[(observed value − predicted value)/observed value]) should be lower than 10%. As far as the PBPK simulations on remifentanil are concerned, AUC values are below this threshold in three out of four predictions. This confirms the quality of the mPBPK model together with the individualization method.

Another important feature of the PBPK model is the capability to gain insight in the elimination pathways of drugs in mammalian body, as shown in Figure 9. This is an important achievement, and can ultimately lead to non-invasive validation of our model when drug and main metabolites in urine and faeces are measured. Future research activity will be devoted to assess the quality of the mPBPK model respect to the oral administration of drugs (preliminary results are reported in Abbiati *et al.*, 2015a,b). The proposed model structure comprises also the oral administration route. Oral bolus transit along the intestine and absorption into blood circulatory system should be considered via the discretization of $SIL$ in a suitable number of perfectly mixed volumes. This involves the active participation of the gastrointestinal tract, which is usually neglected in case of intravenous administration, and calls for the evaluation of the counterdiffusion mass transfer coefficients ($j_{CA}^{SIL}$ and $j_{CA}^{LIL}$). Regarding this last point, we believe it is worth considering these parameters to evaluate the drug reintroduction into the small and large intestinal lumina. In fact, the intestinal wall is not isotropic and, as a result, it seems right to assume that the mass transfer occurs with different direct- and inverse-rate constants through the intestinal membrane.

# Notation

**Abbreviations**

| | | |
|---|---|---|
| ACAT | Advanced Compartmental Absorption and Transit | |
| ADME | Absorption Distribution Metabolism Excretion | |
| AUC | Area Under the Curve | |
| BM | Body Mass | kg |
| BSA | Body Surface Area | m$^2$ |
| CAT | Compartmental Absorption and Transit | |
| CCPK | Classical Compartmental PharmacoKinetics | |
| CPU | Central Process Unit | |
| GICS | Gastrointestinal Circulatory System | |
| GL | Gastric Lumen | |
| IVIVC | *In Vivo/In Vitro* correlation | |

| LIL | Large Intestinal Lumen |
| mPBPK | minimal-PBPK |
| ODE | Ordinary Differential Equation |
| PBPK | Physiologically Based PharmacoKinetics |
| PDE | Partial Differential Equation |
| PK | Pharmacokinetic |
| SD | Standard Deviation |
| SIL | Small Intestinal Lumen |

**Symbols**

| $B$ | Blood flow to different organs | ml/min |
| $C$ | Drug concentration | ng/ml |
| $CL$ | Clearance | ml/min |
| $CO$ | Cardiac Output | l/min |
| $Eff$ | Efficiency | |
| $F$ | Material flow | ng/(ml*min) |
| $IV$ | Intravenous | ng/min |
| $j$ | Mass transfer coefficient | min$^{-1}$ |
| $k$ | Reaction rate constant (metabolism) | min$^{-1}$ |
| $M$ | Mass | ng |
| $PO$ | Drug orally administered (*Per Os*) | ng/min |
| $Q$ | Plasma flow to different organs | ml/min |
| $R$ | Drug bound to protein (expressed as fraction) | |
| $t$ | Time | min |
| $V$ | Volume | cm$^3$ or ml |
| $w$ | Mass fraction | |

**Subscripts**

| ½ | Terminal plasma half-life |
| $A$ | Absorption |
| $CA$ | Counter Absorption |
| $E$ | Elimination |
| $HO-P$ | From Highly perfused Organs to Plasma |
| $MAX$ | Value of the drug peak concentration |
| $P-HO$ | From Plasma to Highly perfused Organs |
| $P-PT$ | From Plasma to Poorly perfused Tissues |
| $PT-P$ | From Poorly perfused Tissues to Plasma |

**Superscripts**

| $GICS$ | Gastrointestinal circulatory system |
| $GL$ | Gastric lumen |
| $H$ | Hepatic |
| $HA$ | Hepatic artery |
| $HO$ | Highly perfused Organs |
| $HV$ | Hepatic vein |
| $K$ | Kidneys |

| | | |
|---|---|---|
| *L* | Liver | |
| *LIL* | Large intestinal lumen | |
| *P* | Plasma | |
| *PT* | Poorly perfused Tissues | |
| *PV* | Portal vein | |
| *SIL* | Small intestinal lumen | |

**Greek letters**

| | | |
|---|---|---|
| *Δ* | Difference | |
| *ρ* | Density | g/ml |

# Acknowledgments

# References

Abbiati, R.A., Cavallaro, G., Craparo, E., Manca, D. (2015a). Sorafenib in mice - A pharmacokinetic study. Chem Eng Trans, 43, 283-288.

Abbiati, R.A., Lamberti, G., Barba, A.A., Grassi, M., Manca, D. (2015b). A PSE approach to patient-individualized physiologically-based pharmacokinetic modeling. Comput Aided Chem Eng, 37, 77-84.

Agoram, B., Woltosz, W.S., & Bolger, M.B. (2001). Predicting the impact of physiological and biochemical processes on oral drug bioavailability. Adv Drug Deliv Rev, 50(1), S41-S67.

Bauer, L.A. (2008). Applied clinical pharmacokinetics ($2^{nd}$ edition). Mc Graw Hill – Medical, USA.

Beers, R., & Camporesi, E. (2004). Remifentanil update: Clinical science and utility. CNS Drugs, 18(15), 1085-1104.

Brown, R.P., Delp, M.D., Lindstedt, S.L., Rhomberg, L.R., & Beliles, R.P. (1997). Physiological parameter values for physiologically based pharmacokinetic models. Toxicol Ind Health. 13(4), 407-484.

Cao, Y., & Jusko, W.J. (2012). Applications of minimal physiologically-based pharmacokinetic models. J Pharmacokinet Pharmacodyn, 39(6), 711-723.

Cowles, A.L., Borgstedt, H.H., & Gillies, A.J. (1971). Tissue weights and rates of blood flow in man for the prediction of anesthetic uptake and distribution. Anesthesiology, 35(5), 523-526.

Del Cont, R., Abrami, M., Hasa, D., Perissutti, B., Voinovich, B., Barba, A., Lamberti, G., Grassi, G., Colombo, I., Manca, D., & Grassi, M. (2014). A physiologically-oriented mathematical model for the description of in vivo drug release and absorption. ADMET & DMPK, 2(2), 80-97.

Dershwitz, M., Hoke, J.F., Rosow, C.E., Michałowski, P., Connors, P.M., Muir, K.T., & Dienstag, J.L. (1996). Pharmacokinetics and pharmacodynamics of remifentanil in volunteer subjects with severe liver disease. Anesthesiology, 84(4), 812-820.

Di Muria, M., Lamberti, G., & Titomanlio, G. (2010). Physiologically based pharmacokinetics: A simple, all purpose model. Ind Eng Chem Res, 49(6), 2969-2978.

Duthie, D.J.R. (1998). Remifentanil and tramadol. Br J Anaesth, 81(1), 51-57.

Egan, T.D. (2000). Pharmacokinetics and pharmacodynamics of remifentanil: An update in the year 2000. Curr Opin Anaesthesiol, 13(4), 449-455.

Egan, T.D. (2003). Target-controlled drug delivery: Progress toward an intravenous "vaporizer" and automated anesthetic administration. Anesthesiology, 99(5), 1214-1219.

Egan, T.D., Lemmens, H.J.M., Fiset, P., Hermann, D.J., Stanski, D.R., & Shafer, S.L. (1993). The pharmacokinetics of the new short-acting opioid remifentanil (GI87084B) in healthy adult male volunteers. Anesthesiology, 79(5), 881-892.

FDA, (1997). Guidance for industry: extended release oral dosage forms: development, evaluation, and application of in vitro/in vivo correlations, Center for Drug Eval. and Research (CDER).

Grassi, G., Hasa, D., Voinovich, D., Beatrice Perissutti, B., Dapas, B., Farra, R., Franceschinis, E., & Grassi, M. (2010). Simultaneous Release and ADME Processes of Poorly Water-Soluble Drugs: Mathematical Modeling. Mol. Pharmaceutics, 7(5), 1488 – 1497.

Gueorguieva, I., Nestorov, I.A., & Rowland, M. (2006). Reducing whole body physiologically based pharmacokinetic models using global sensitivity analysis: Diazepam case study. J Pharmacokinet Pharmacodyn, 33(1), 1-27.

Heitzig, M., Linninger, A.A., Sin, G., & Gani, R. (2014). A computer-aided framework for development, identification and management of physiologically-based pharmacokinetic models. Comput Chem Eng, 71, 677-698.

Himmelstein, K.J. & Lutz, R.J. (1979). A review of the applications of physiologically based pharmacokinetic modeling. J Pharmacokinet Biopharm, 7(2), 127-145.

Huang, S-M., Abernethy, D.R., Wang, Y., Zhao, P., & Zineh, I. (2013). The utility of modeling and simulation in drug development and regulatory review. J Pharm Sci, 102(9), 2912-2923.

Jain, R., Gerlowski, L.E., Weissbrod, J.M., Wang, J., & Pierson, R.N. (1981). Kinetics of uptake, distribution end excretion of zinc in rats. Ann Biomed Eng, 9, 347-361.

Jones, H.M., & Rowland-Yeo, K. (2013). Basic concepts in physiologically based pharmacokinetic modeling in drug discovery and development. CPT Pharmacometrics Syst Pharmacol, 2(8), e63.

Laínez-Aguirre, J.M., Blau, G.E., Mockus, L., Orçun, S., & Reklaitis, G.V. (2011). Pharmacokinetic based design of individualized dosage regimens using a bayesian approach. Ind Eng Chem Res, 50, 5114-5130.

Laínez-Aguirre, J.M., Blau, G.E., & Reklaitis, G.V. (2014). Postulating compartmental models using a flexible approach. Comput Aided Chem Eng, 33, 1171-1176.

Lindstedt, S.L., & Schaeffer, P.J. (2002). Use of allometry in predicting anatomical and physiological parameters of mammals. Lab Anim, 36 (1), 1-19.

Mordenti, J. (1986). Man versus Beast: Pharmacokinetic Scaling in Mammals. J Pharm Sci, 75(11), 1028-1040.

Morse, B. L., & Kim, R. B. (2015). Is personalized medicine a dream or a reality?. Crit Rev Clin Lab Sci, 52, 1-11.

Mošat', A., Lueshen, E., Heitzig, M., Hall, C., Linninger, A.A., Sin, G., & Gani, R. (2013). First principles pharmacokinetic modeling: A quantitative study on cyclosporin. Comput Chem Eng, 54, 97-110.

Nestorov, I.A., Aarons, L.J., Arundel, P.A., & Rowland, M. (1998). Lumping of whole-body physiologically based pharmacokinetic models. J Pharmacokinet Biopharm, 26(1), 21-46.

Ongoiba, N., Sissoko, F., Ouologuem, I., Berete, S., Traore, A.K., Sidibe, S., Toure, M., Keita, A.D., & Koumare, A.K. (2003). Portal vein: echographic anatomy. Morphologie, 87(277), 29-32.

Pavurala, N., & Achenie, L.E.K. (2013). A mechanistic approach for modeling oral drug delivery. Comput Chem Eng, 57, 196-206.

Pilari, S., & Huisinga, W. (2010). Lumping of physiologically-based pharmacokinetic models and a mechanistic derivation of classical compartmental models. J Pharmacokinet Pharmacodyn, 37(4), 365-405.

Pitsiu, M., Wilmer, A., Bodenham, A., Breen, D., Bach, V., Bonde, J., Kessler, P., Albrecht, S., Fisher, G., & Kirkham, A. (2004). Pharmacokinetics of remifentanil and its major metabolite, remifentanil acid, in ICU patients with renal impairment. Br J Anaesth, 92(4), 493-503

Teorell, T. (1937). Kinetic of distribution of substances administered to the body II. The intravascular modes of administration. Arch Int Pharmacodyn, 57, 226-240.

Tortora, G.J., Nielsen M.T. (2014). Principles of human anatomy (13th edition). Wiley, USA.

Wagner, J.G. (1981). History of Pharmacokinetics. Pharmacol Therapeut, 12, 537-562.

Wagner, J.G. (1993). Pharmacokinetics for the pharmaceutical scientist. Technomic, Lancaster (USA).

Weinreb, J., Kumari, S., Phillips, G., & Pochaczevsky, R. (1982). Portal vein measurements by real-time sonography. Am J Roentgenol, 139(2), 497-499.

Westmoreland, C.L., Hoke, J.F., Sebel, P.S., Hug, Jr. C.C., & Muir, K.T. (1993). Pharmacokinetics of remifentanil (GI87084B) and its major metabolite (GI90291) in patients undergoing elective inpatient surgery. Anesthesiology, 79(5), 893-903.

Williams, L.R., & Leggett, R.W. (1989). Reference values for resting blood flow to organs of man. Clin Phys Physiol Meas, 10(3), 187-217.

Yu, L.X., & Amidon, G.L. (1998). Saturable small intestinal drug absorption in humans: Modeling and interpretation of cefatrizine data. Eur J Pharm Biopharm, 45(2), 199-203.

Yu, L.X., & Amidon, G.L. (1999). A compartmental absorption and transit model for estimating oral drug absorption. Int J Pharm, 186(2), 119-125.

Yu, L.X., Crison, J.R., & Amidon, G.L. (1996b). Compartmental transit and dispersion model analysis of small intestinal transit flow in humans. Int J Pharm, 140(1), 111-118.

Yu, L.X., Lipka, E., Crison, J.R., & Amidon G.L. (1996a). Transport approaches to the biopharmaceutical design of oral drug delivery systems: Prediction of intestinal absorption. Adv Drug Deliver Rev, 19(3), 359-376.

Zhao, P., Rowland, M., & Huang, S-M. (2012). Best practice in the use of physiologically based pharmacokinetic modeling and simulation to address clinical pharmacology regulatory questions. Clin Pharmacol Ther, 92(1), 17-20.